

A hole accelerator for InGaN/GaN light-emitting diodes

Zi-Hui Zhang, Wei Liu, Swee Tiam Tan, Yun Ji, Liancheng Wang, Binbin Zhu, Yiping Zhang, Shunpeng Lu, Xueliang Zhang, Namig Hasanov, Xiao Wei Sun, and Hilmi Volkan Demir

Citation: *Applied Physics Letters* **105**, 153503 (2014); doi: 10.1063/1.4898588

View online: <http://dx.doi.org/10.1063/1.4898588>

View Table of Contents: <http://scitation.aip.org/content/aip/journal/apl/105/15?ver=pdfcov>

Published by the *AIP Publishing*

Articles you may be interested in

[p-doping-free InGaN/GaN light-emitting diode driven by three-dimensional hole gas](#)

Appl. Phys. Lett. **103**, 263501 (2013); 10.1063/1.4858386

[The effect of silicon doping in the barrier on the electroluminescence of InGaN/GaN multiple quantum well light emitting diodes](#)

J. Appl. Phys. **114**, 103102 (2013); 10.1063/1.4820450

[Enhanced overall efficiency of GaInN-based light-emitting diodes with reduced efficiency droop by Al-composition-graded AlGaIn/GaN superlattice electron blocking layer](#)

Appl. Phys. Lett. **103**, 061104 (2013); 10.1063/1.4817800

[Influence of n-type versus p-type AlGaIn electron-blocking layer on InGaN/GaN multiple quantum wells light-emitting diodes](#)

Appl. Phys. Lett. **103**, 053512 (2013); 10.1063/1.4817381

[AlGaInN-based ultraviolet light-emitting diodes grown on Si\(111\)](#)

Appl. Phys. Lett. **80**, 3682 (2002); 10.1063/1.1480886

The advertisement features a blue background with a film strip graphic on the left. The text is in white and orange. The Oxford Instruments logo is in the bottom right corner.

Not all AFMs are created equal
Asylum Research Cypher™ AFMs
There's no other AFM like Cypher

www.AsylumResearch.com/NoOtherAFMLikeIt

OXFORD
INSTRUMENTS
The Business of Science®

A hole accelerator for InGaN/GaN light-emitting diodes

Zi-Hui Zhang,¹ Wei Liu,¹ Swee Tiam Tan,¹ Yun Ji,¹ Liancheng Wang,¹ Binbin Zhu,¹ Yiping Zhang,¹ Shunpeng Lu,¹ Xueliang Zhang,¹ Namig Hasanov,¹ Xiao Wei Sun,^{1,a)} and Hilmi Volkan Demir^{1,2,a)}

¹LUMINOUS! Centre of Excellence for Semiconductor Lighting and Displays, School of Electrical and Electronic Engineering, School of Physical and Mathematical Sciences, Nanyang Technological University, 50 Nanyang Avenue, Singapore 639798

²Department of Electrical and Electronics, Department of Physics, and UNAM-Institute of Material Science and Nanotechnology, Bilkent University, TR-06800 Ankara, Turkey

(Received 15 September 2014; accepted 6 October 2014; published online 15 October 2014)

The quantum efficiency of InGaN/GaN light-emitting diodes (LEDs) has been significantly limited by the insufficient hole injection, and this is caused by the inefficient p-type doping and the low hole mobility. The low hole mobility makes the holes less energetic, which hinders the hole injection into the multiple quantum wells (MQWs) especially when a p-type AlGaIn electron blocking layer (EBL) is adopted. In this work, we report a hole accelerator to accelerate the holes so that the holes can obtain adequate kinetic energy, travel across the p-type EBL, and then enter the MQWs more efficiently and smoothly. In addition to the numerical study, the effectiveness of the hole accelerator is experimentally shown through achieving improved optical output power and reduced efficiency droop for the proposed InGaN/GaN LED. © 2014 AIP Publishing LLC.

[<http://dx.doi.org/10.1063/1.4898588>]

As a promising lighting source, high-efficiency GaN-based light-emitting diodes (LEDs) have attracted extensive interest so far.^{1,2} However, the development of the GaN-based LEDs is still substantially hindered by the efficiency droop, a notorious phenomenon, due to which the quantum efficiency of LEDs is reduced as the injection current level is elevated.³ Suggested mechanisms for the efficiency droop include Auger recombination,⁴ strong electron overflow,⁵ and low injection efficiency for holes.⁶ To suppress the aforementioned mechanisms for the efficiency droop, several remedies have been proposed and demonstrated. It has been well established that Auger recombination can be suppressed by flattening the energy band of the quantum wells and reducing the local carrier density.^{7,8} Meanwhile, in order to reduce the electron leakage level, approaches such as the polarization matched InAlN p-type electron blocking layer (EBL) and a polarization self-screened p-type AlGaIn EBL⁹ have been utilized to replace the conventional p-type AlGaIn EBL.¹⁰ Besides the commonly adopted p-type EBLs, hot electrons can be further cooled down by using an InGaIn electron cooler layer¹¹ or a n-type AlGaIn EBL.¹² The quantum barriers can also be further optimized by growing thin AlGaInN cap layers to enhance the electron injection efficiency.¹³ Nevertheless, thanks to the proposed electron blocking structures, the electron leakage can be significantly suppressed but it cannot be completely eliminated. It is advisable to enhance the hole injection efficiency into the InGaN/GaN multiple quantum wells (MQWs) so that the non-equilibrium electrons can recombine with the injected holes, and the electron leakage rate can be further reduced.⁹ For that reason, tremendous effort has thus been made to improve the hole injection efficiency into the MQWs.

Examples of the proposed strategies rely on improving the hole injection capability by properly thinning the quantum barriers,^{14,15} by using p-type doped quantum barriers¹⁶ and by employing the multiple interband tunnel junctions to link the tandem MQWs.¹⁷ All these designs target at homogenizing the hole distribution within the active region. However, current LED architectures normally adopt a p-type EBL to reduce the electron leakage, and this inevitably blocks the hole injection due to the valance band offset between the p-type EBL and the p-GaN layer. Therefore, the essence of enhancing the hole injection efficiency is to promote the hole transport across the p-type EBL.⁶ In this work, different from the previous reports, we propose and develop a hole accelerator to energize the holes so that the holes obtain kinetic energy to climb over the p-type EBL.

The physical model of the hole accelerator can be elaborated as follows. Those holes having excess energy of $E \geq \max\{0, (\phi_{EBL} - E_k)\}$ (where ϕ_{EBL} is the valance band barrier height between the p-type EBL and p-GaN for holes, E_k is the kinetic energy of the holes) are able to travel across the p-EBL. If we assume that the holes in the p-GaN layer follow the Fermi-Dirac $[F(E)]$ distribution, then the probability of finding the holes in the last quantum barrier is $P_h = \int_{E \geq \max\{0, (\phi_{EBL} - E_k)\}}^{+\infty} F(E) \cdot P(E) dE / \int_0^{+\infty} F(E) \cdot P(E) dE$, where $P(E)$ represents the valance band density of states in the p-GaN layer. Thus, P_h will be enhanced if $(\phi_{EBL} - E_k)$ is smaller, which can be realized through reducing ϕ_{EBL} or increasing E_k . The ϕ_{EBL} can be reduced by decreasing the AlN composition in the p-type EBL. However, this approach may aggravate the electron leakage rate due to the simultaneous reduction in the conduction band offset between the last quantum barrier and the p-type EBL. Hence, one promising way to reduce $(\phi_{EBL} - E_k)$ is to make E_k higher for holes. Nevertheless, it is also known that $E_k = \frac{1}{2} m_h^* \cdot V^2$, while $V = \mu_p \cdot E_{field}$. Here, V is the hole velocity, μ_p is the hole

^{a)}Electronic addresses: EXWSUN@ntu.edu.sg and VOLKAN@stanfordalumni.org

mobility, m_h^* is the effective mass for holes, and E_{field} is the electric field, by which the holes are accelerated/decelerated.¹⁸ Thus, it is unambiguous that one can energize the holes by manipulating the mobility and the electric field. The carrier mobility can be improved by reducing the doping level of the p-GaN layer. However, the hole mobility for p-GaN layer is typically lower than $10 \text{ cm}^2/\text{V s}$, hence there is little room to further increase the hole mobility. Nevertheless, the hole velocity can also be adjusted by varying the electric field profile. As well-known, III-nitride epitaxial films grown along the [0001] (i.e., C+) orientation possess a very strong polarization induced electric field.¹⁹ This can be employed to accelerate the holes. Through a hole accelerator, holes can be made more energetic or “hotter.” The schematic energy band diagram for the hole accelerator is shown in Fig. 1, where the hole accelerator comprises two p-GaN layers (L1 and L3) and a p-AlGaN layer (L2). The polarization induced interface charges are also represented in Fig. 1. The holes are injected from layer L1 and reach layer L3 by travelling across layer L2. In order to reduce the hole blocking effect at the interface of layers L1 and L2, the p-AlGaN layer has to be properly thin. Once the holes arrive at layer L3, they will receive the additional energy from the polarization induced electric field in layer L3 and become “hot.”

To prove the effectiveness of the hole accelerator in promoting the hole injection efficiency, two LED samples (LEDs A and B) were grown by a metal-organic chemical vapor deposition (MOCVD) system. The growth was initiated on planar C-plane sapphire substrates. A 20 nm thick GaN buffer layer was firstly grown before the $4 \mu\text{m}$ thick unintentionally n-type GaN (u-GaN) layer. A $2 \mu\text{m}$ thick Si-doped n-GaN was subsequently grown as the electron injection layer of which the Si doping concentration is $5 \times 10^{18} \text{ cm}^{-3}$ with the diluted SiH_4 serving as the dopant precursor. Then, five-period $\text{In}_{0.15}\text{Ga}_{0.85}\text{N}/\text{GaN}$ MQWs were grown with the well thickness and barrier thickness of 3 and 12 nm, respectively. The MQW was capped by a 25 nm thick p-type $\text{Al}_{0.20}\text{Ga}_{0.80}\text{N}$ EBL. For LED A, a p-GaN of $0.2 \mu\text{m}$ thickness was grown working as the hole

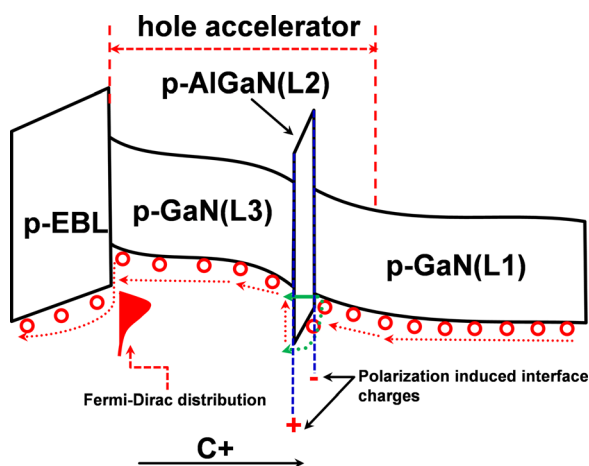


FIG. 1. Schematic energy diagram of the proposed accelerator. Solid green arrow and dashed green one illustrate the hole transport through intraband tunneling and thermionic emission, respectively.

source region. However, LED B differs from LED A in the hole source layer by incorporating the hole accelerator. The hole accelerator was grown directly after the p-type EBL, and the growth details are as follows: a 80 nm thick p-GaN layer was grown first and a thin 3 nm thick p- $\text{Al}_{0.25}\text{Ga}_{0.75}\text{N}$ layer then followed, which provides the polarization induced interface charges as shown in Fig. 1 and realizes the acceleration effect to holes. It is worth mentioning that we purposely make the p- $\text{Al}_{0.25}\text{Ga}_{0.75}\text{N}$ layer thin so that the hole blocking effect can be mitigated. Next, another 120 nm p-GaN was grown after the p- $\text{Al}_{0.25}\text{Ga}_{0.75}\text{N}$ layer in LED B. Here, CP_2Mg was utilized as the precursor for the p-type dopant. The hole concentration for all the p-type layers here was estimated to $3 \times 10^{17} \text{ cm}^{-3}$ by considering a 1% ionization efficiency for Mg dopants at room temperature. Furthermore, both the p-type $\text{Al}_{0.20}\text{Ga}_{0.80}\text{N}$ and p-type $\text{Al}_{0.25}\text{Ga}_{0.75}\text{N}$ layers were grown at 100 mbars. Lastly, LEDs A and B were both covered with a 20 nm thick heavily p-type doped (p^+) GaN layer to facilitate the ohmic contact with metal electrodes.

Electroluminescence (EL) was measured for the grown LED samples by an integrating sphere attached to an Ocean Optics spectrometer (QE65000). The size of the tested LED dies is $1 \times 1 \text{ mm}^2$ with indium bump used as the ohmic contact. The EL spectra at 10, 30, 50, and 70 A/cm^2 are presented in Figs. 2(a) and 2(b) for LEDs A and B, respectively. The peak emission wavelength for the two LEDs is both $\sim 455 \text{ nm}$, which reflects that the epitaxial growth of the hole accelerator did not affect the quantum well configuration for LED B. The red shift of the emission wavelength observed as the injected current level increases for both LEDs is attributed to the accumulated junction heat during the electrical operation.²⁰ Moreover, the EL intensity for LED B is substantially higher than that for LED A only when the current density exceeds 30 A/cm^2 , and the reason of such phenomena will be discussed subsequently.

Along with the EL spectra, the corresponding optical output power density and the external quantum efficiency (EQE) at various injection current levels for LEDs A and B have also been measured and demonstrated in Fig. 3. The optical output power densities for LEDs A and B at 100 A/cm^2 are ~ 31.4 and $\sim 36.1 \text{ W/cm}^2$, respectively, showing a performance enhancement of $\sim 15.0\%$. On the other hand, a suppressed efficiency droop has also been obtained from LED B. The droop levels [$\text{droop} = (EQE_{\text{max}} - EQE_{\text{test}})/EQE_{\text{max}}$] at 100 A/cm^2 for LEDs A and B are $\sim 54.2\%$ and $\sim 35.9\%$, respectively. Since the two LEDs are identical to each other in their electron injection layers, MQWs and the p-type EBL, except the hole accelerator, the electron transport is less likely to be affected in the proposed design. Therefore, the different levels of optical performance shall be attributed to the different hole injection efficiencies of the two LEDs, and an elevated hole injection efficiency is favored by the hole accelerator in LED B. It is worthy of noting that the EQE for LED B is lower than that for LED A when the current density is smaller than $\sim 10 \text{ A/cm}^2$, which can be observed from Figs. 2(a) and 2(b). The unimproved optical performance for LED B at the low current injection levels ($< 10 \text{ A/cm}^2$) is most likely due to the blocking effect by the p- $\text{Al}_{0.25}\text{Ga}_{0.75}\text{N}$ layer in the hole accelerator region.

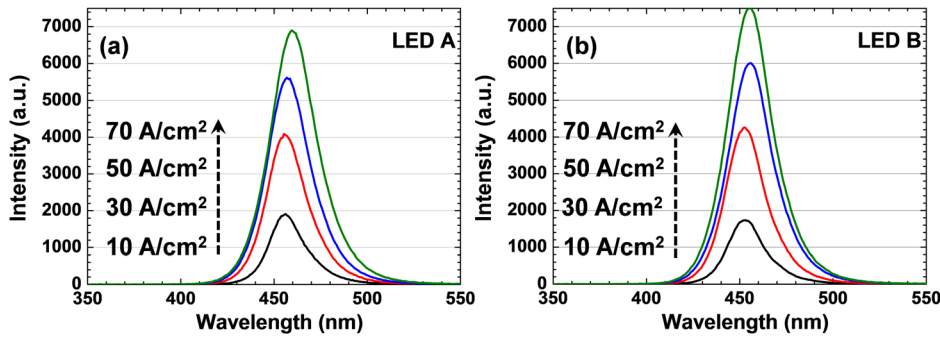


FIG. 2. EL spectra collected at 10, 30, 50, and 70 A/cm^2 for (a) LED A and (b) LED B.

Besides the physical model and experimental proof of the hole accelerator in making the holes “hot” and promoting the hole injection across the p-type EBL, it is also essential to numerically reveal and precisely study the physical picture for the functions of the hole accelerator in terms of the energy band profiles and the hole distribution in the MQW region. For this purpose, the numerical computations were conducted by a commercial simulation package of APSYS,⁹ while the physical models were properly set by users. Important physical parameters such as the energy band offset ratio of the MQW, Auger recombination coefficient and Shockley-Read-Hall recombination coefficient can be found in our previously published works.^{2-5,11,14,16} Specifically, we assumed a 50/50 energy band offset ratio for the AlGaN/GaN heterostructures in our LEDs.³ The polarization effect is represented by properly setting the polarization interface charges at each heterojunction.¹⁹ To take into account the crystal relaxation by dislocation generation, we assumed a 40% polarization level in our calculations.^{2-5,11,14,16} The computations treat each heterojunction as a rectangular barrier and both the thermionic emission and thermally assisted intraband tunneling processes are considered when calculating the carrier transport. According to the room-temperature Hall measurement (not shown here) for our grown LED samples, in our computations, we set a constant hole mobility of $\sim 5.0 \text{ cm}^2/\text{V}\cdot\text{s}$ for both the p-GaN and p-AlGaN layers, which have the hole concentration of $\sim 3 \times 10^{17} \text{ cm}^{-3}$. We set constant hole mobility, as neglecting the dependence of hole mobility on the magnitude of the electric field will not change our conclusion for III-nitride optoelectronic devices.²¹

The computed energy band diagram comprising the p-type $\text{Al}_{0.20}\text{Ga}_{0.80}\text{N}$ EBL and the partial p-GaN layer for

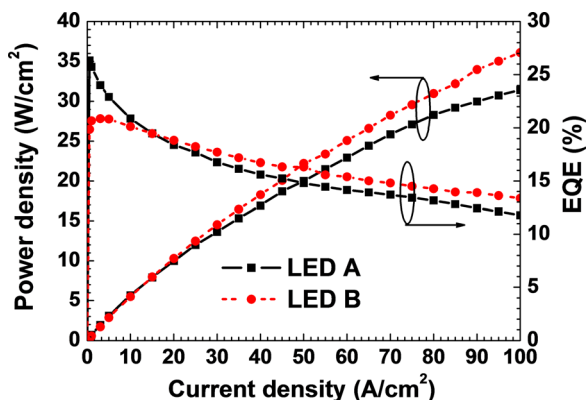


FIG. 3. Experimentally measured optical output power density and EQE as a function of the injection current density for LEDs A and B.

LED A is shown in Fig. 4(a), while Fig. 4(b) shows the energy band diagram for the p-type $\text{Al}_{0.20}\text{Ga}_{0.80}\text{N}$ EBL and the hole accelerator for LED B. The energy band of the p-GaN layer is flat for LED A, and hence the holes can only be accelerated by the external electrical bias. However, when a thin p- $\text{Al}_{0.25}\text{Ga}_{0.75}\text{N}$ layer is embedded into the p-GaN region, the strong polarization effect at the p- $\text{Al}_{0.25}\text{Ga}_{0.75}\text{N}/\text{p-GaN}$ heterojunction significantly bends the energy band such that the holes have an energy difference when entering L3 from L1 (refer to Fig. 1). Such a band bending makes the holes more energetic and “hotter” when they reach the p-type $\text{Al}_{0.20}\text{Ga}_{0.80}\text{N}$ EBL.

To better interpret the hole acceleration effect, we further present the electric field profile of the hole accelerator for LED B in Fig. 4(c). The electric field profile at the corresponding position for LED A is also included for comparison. The positive direction of the electric field profile in Fig. 4(c) is along the C^+ orientation. Hence, the holes will be decelerated when they enter the p- $\text{Al}_{0.25}\text{Ga}_{0.75}\text{N}$ layer, requiring that the thickness of the p- $\text{Al}_{0.25}\text{Ga}_{0.75}\text{N}$ layer has to be properly adjusted. However, holes will be accelerated when transporting in the left p-GaN region (i.e., L3 in Fig. 1). The net work done to the holes during the whole transportation from L1 to L3 by the electric field can be written as $W = e \int_0^l E_{\text{field}} \cdot dx$. In this work, for a comparative study, the integration range starts from the interface of the p-type EBL and the neighboring p-GaN and ends at the relative position of $0.72 \mu\text{m}$ as shown in Fig. 4, since beyond this range the electric field for LEDs A and B are identical. The integration step (dx) has been properly set through optimizing the mesh distribution in the simulated devices. The calculated results show that W is 0.087 eV and 1.069 eV for LEDs A and B at $100 \text{ A}/\text{cm}^2$, respectively, and this indicates that the holes in LED B will acquire more energy and become more energetic than those in LED A before reaching the p-type EBL. Those more energized holes have a higher probability of climbing over the p-type EBL and entering the MQW region. Note that in LED B, those thermionic emitted holes will lose energy with the amount of the valance band offset between p- $\text{Al}_{0.25}\text{Ga}_{0.75}\text{N}$ and p-GaN layers (ΔE_v). However, such energy loss of ΔE_v will be recovered back once the holes transport to the left p-GaN layer (i.e., L3 in Fig. 1) from the p- $\text{Al}_{0.25}\text{Ga}_{0.75}\text{N}$ region. As a result, there is no impact of the valance band discontinuity of ΔE_v on the hole kinetic energy.

The hole concentration profiles for LEDs A and B are also computed and presented in Fig. 5 at $100 \text{ A}/\text{cm}^2$. According to the aforementioned calculations, compared to

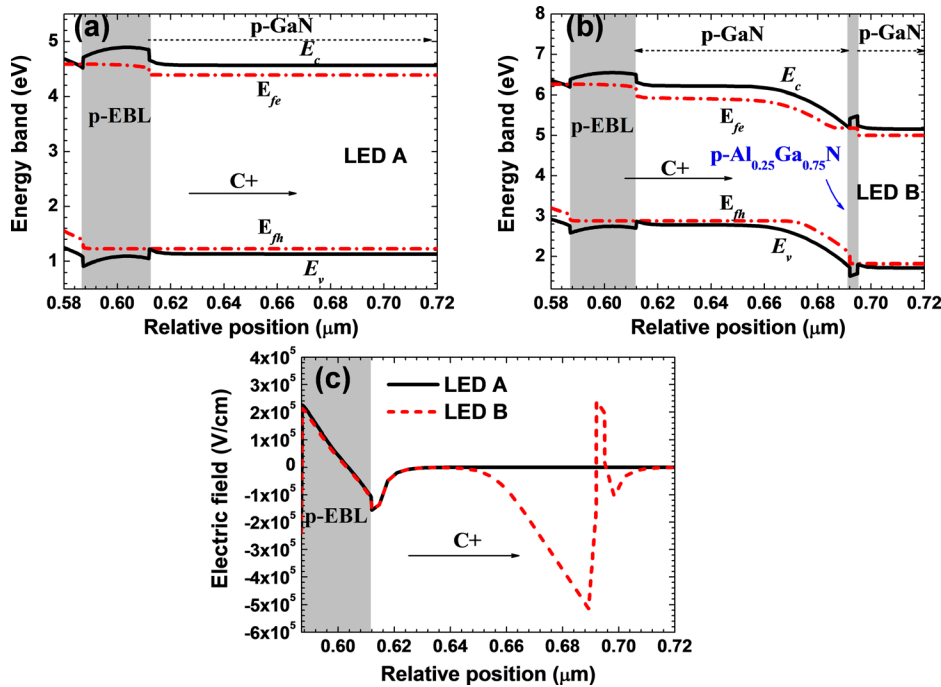


FIG. 4. Calculated energy band diagrams for (a) LED A and (b) LED B, and (c) the electric field profiles within the hole accelerator region for the two LEDs. Data were collected at 100 A/cm^2 . E_c , E_v , E_{fe} , and E_{fh} denote the conduction band, valence band, and quasi-Fermi level for electrons and for holes, respectively. The positive direction of the electric field is along the C+ orientation.

LED A, holes in LED B will receive more additional energy due to the hole accelerator. The more energetic holes guarantee a smoother and more efficient injection into the quantum wells. As a result, the hole concentration in the quantum wells for LED B is higher than that for LED A, as is shown in Fig. 5. The uneven hole concentration in different quantum wells can be further homogenized by doping the quantum barriers with proper Mg dosage¹⁶ or properly thinning the quantum barrier thickness.^{14,15}

In conclusion, in this work we have proposed and demonstrated a concept of hole accelerator. By using it, the holes will be energized as a result of the polarization induced electric field within the hole accelerator. Those “hot” holes have an enhanced probability of traveling across the p-type electron blocking layer and being more smoothly injected into the active region of a light-emitting diode. The hole accelerator has also been experimentally proven to be very useful in enhancing the optical output power and relieving the efficiency droop for light-emitting diodes. Assisted by the powerful numerical calculation tools, an increased hole concentration has been observed in the quantum wells for the

light-emitting diode with the hole accelerator. The hole accelerator holds great promise for achieving high-efficiency solid-state lighting devices.

This work was supported by the National Research Foundation of Singapore under Grant Nos. NRF-CRP-6-2010-2, NRF-CRP11-2012-01, and NRF-RF-2009-09 and the Singapore Agency for Science, Technology and Research (A*STAR) SERC under Grant No. 112 120 2009.

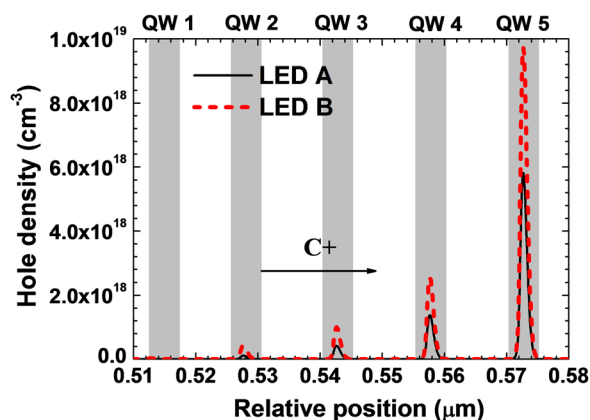


FIG. 5. Calculated hole concentration in LEDs A and B at 100 A/cm^2 .

- ¹N. Tansu, H. Zhao, G. Liu, X. H. Li, J. Zhang, H. Tong, and Y. K. Ee, *IEEE Photonics J.* **2**, 241 (2010).
- ²S. T. Tan, X. Sun, H. V. Demir, and S. DenBaars, *IEEE Photonics J.* **4**, 613 (2012).
- ³J. Piprek, *Phys. Status Solidi A* **207**, 2217 (2010).
- ⁴J. Iveland, L. Martinelli, J. Peretti, J. S. Speck, and C. Weisbuch, *Phys. Rev. Lett.* **110**, 177406 (2013).
- ⁵M.-H. Kim, M. F. Schubert, Q. Dai, J. K. Kim, E. F. Schubert, J. Piprek, and Y. Park, *Appl. Phys. Lett.* **91**, 183507 (2007).
- ⁶Z.-H. Zhang, Z. Ju, W. Liu, S. T. Tan, Y. Ji, Z. Kyaw, X. Zhang, N. Hasanov, X. W. Sun, and H. V. Demir, *Opt. Lett.* **39**, 2483 (2014).
- ⁷R. Vaxenburg, A. Rodina, E. Lifshitz, and A. L. Efros, *Appl. Phys. Lett.* **103**, 221111 (2013).
- ⁸Z.-H. Zhang, W. Liu, Z. Ju, S. T. Tan, Y. Ji, Z. Kyaw, X. Zhang, L. Wang, X. W. Sun, and H. V. Demir, *Appl. Phys. Lett.* **105**, 033506 (2014).
- ⁹Z.-H. Zhang, W. Liu, Z. Ju, S. Tiam Tan, Y. Ji, X. Zhang, L. Wang, Z. Kyaw, X. W. Sun, and H. V. Demir, *Appl. Phys. Lett.* **104**, 251108 (2014).
- ¹⁰S. Choi, H. J. Kim, S.-S. Kim, J. Liu, J. Kim, J.-H. Ryou, R. D. Dupuis, A. M. Fischer, and F. A. Ponce, *Appl. Phys. Lett.* **96**, 221105 (2010).
- ¹¹Z.-H. Zhang, W. Liu, S. T. Tan, Z. Ju, Y. Ji, Z. Kyaw, X. Zhang, N. Hasanov, B. Zhu, S. Lu, Y. Zhang, X. W. Sun, and H. V. Demir, *Opt. Express* **22**, A779–A789 (2014).
- ¹²Z.-H. Zhang, Y. Ji, W. Liu, S. Tiam Tan, Z. Kyaw, Z. Ju, X. Zhang, N. Hasanov, S. Lu, Y. Zhang, B. Zhu, X. W. Sun, and H. V. Demir, *Appl. Phys. Lett.* **104**, 073511 (2014).
- ¹³G. Liu, J. Zhang, C. K. Tan, and N. Tansu, *IEEE Photonics J.* **5**, 2201011 (2013).
- ¹⁴M.-C. Tsai, S.-H. Yen, Y.-C. Lu, and Y.-K. Kuo, *IEEE Photonics Technol. Lett.* **23**, 76 (2011).
- ¹⁵Z. Ju, W. Liu, Z.-H. Zhang, S. T. Tan, Y. Ji, Z. Kyaw, X. Zhang, S. Lu, Y. Zhang, and B. Zhu, *Appl. Phys. Lett.* **102**, 243504 (2013).
- ¹⁶Y. Ji, Z.-H. Zhang, S. T. Tan, Z. G. Ju, Z. Kyaw, N. Hasanov, W. Liu, X. W. Sun, and H. V. Demir, *Opt. Lett.* **38**, 202 (2013).
- ¹⁷J. Piprek, *Appl. Phys. Lett.* **104**, 051118 (2014).

¹⁸S. M. Sze, *Physics of Semiconductor Devices*, 2nd ed. (John Wiley & Sons, Inc., 1981).

¹⁹V. Fiorentini, F. Bernardini, and O. Ambacher, *Appl. Phys. Lett.* **80**, 1204 (2002).

²⁰Z. Gong, S. Jin, Y. Chen, J. McKendry, D. Massoubre, I. M. Watson, E. Gu, and M. D. Dawson, *J. Appl. Phys.* **107**, 013103 (2010).

²¹J. Piprek, R. K. Sink, M. A. Hansen, J. E. Bowers, and S. P. DenBaars, *Proc. SPIE* **3944**, 28 (2000).